# TOAST: Fast and scalable auto-partitioning based on principled static analysis

Sami Alabed\*

Google DeepMind London, UK

Timur Sitdikov\*

Google DeepMind London, UK Dominik Grewe\*†

Isomorphic Labs London, UK

Agnieszka Swietlik\*

Google DeepMind London, UK

**Daniel Belov** 

Google DeepMind London, UK

1

Norman A. Rink\*

Google DeepMind London, UK

Dimitrios Vytiniotis\*

Google DeepMind London, UK

### **Abstract**

Partitioning large machine learning models across distributed accelerator systems is a complex process, requiring a series of interdependent decisions that are further complicated by internal sharding ambiguities. Consequently, existing autopartitioners often suffer from out-of-memory errors or are prohibitively slow when exploring the exponentially large space of possible partitionings. To mitigate this, they artificially restrict the search space, but this approach frequently yields infeasible solutions that violate device memory constraints or lead to sub-optimal performance.

We propose a system that combines a novel static compiler analysis with a Monte Carlo Tree Search. Our analysis constructs an efficient decision space by identifying (i) tensor dimensions requiring identical sharding, and (ii) partitioning "conflicts" that require resolution.

Our system significantly outperforms state-of-the-art industrial methods across diverse hardware platforms and model architectures, discovering previously unknown, superior solutions, and the process is fully automated even for complex and large models.

#### 1 Introduction

The increasing size of machine learning (ML) models necessitates training on distributed systems of accelerator devices (e.g., GPUs, TPUs [8, 17, 18]). This distributed approach is required because the memory footprints of model parameters and input data routinely exceed the capacity of a single device. Consequently, ML engineers face the significant challenge of adapting their model code for execution on these distributed systems. Manually converting code that defines the mathematics of a model to semantically equivalent code that executes on a distributed system is time-consuming, highly error prone and simply does not scale with model size

and complexity. To assist with this challenge, a number of partitioning tools [2, 22, 37, 45] have emerged. These tools typically take in ML code in a domain-specific language (e.g. TensorFlow [1], JAX [5], PyTorch [30]) and, usually at the level of an intermediate representation (IR), rewrite code for local device execution, inserting cross-device communication. This local code operates on partitioned tensors, specifically the *shards* of inputs and model parameters residing on each device. While these tools automate the mechanics of partitioning a model, users are still responsible for determining the optimal sharding strategy. This requires deciding which tensors to partition based on the model architecture, tensor dimensions, and device topology. Developing optimal partitioning strategies requires significant engineering effort [11, 20, 31, 32, 38, 46]. Consequently, many new model architectures lack well-established partitioning strategies.

Automatic partitioning tools [36, 47] have emerged to discover partitioning strategies for ML models. These tools operate by exploring the search space of possible model partitionings, guided by a performance model that estimates the runtime of each configuration. This search space is exponential in the number of model operations as it comprises all possible sharding combinations for every tensor. Even for models represented in a high-level intermediate representation (IR) like StableHLO [29], this involves tens of thousands of operations, making exhaustive exploration intractable. For instance, Alpa [47] considers every tensor as a candidate for sharding, creating a large search space, which leads to slow compilation times and yields sub-optimal solutions. AutoMap [3, 36] addresses this challenge by combining explicit sharding decisions, exposed in the search space, with implicit compiler-driven propagation of those decisions to the rest of the model. However, this approach relies on the user to manually specify key locations in the model where resharding might be beneficial (e.g., for collective communication in transformer sequence parallelism [20]). Therefore, auto-partitioners must aggressively prune the search space without discarding good solutions.

<sup>\*</sup>Equal contribution, authors in alphabetical order. Correspondence to: dvytin@google.com

<sup>†</sup>Work done while at Google DeepMind

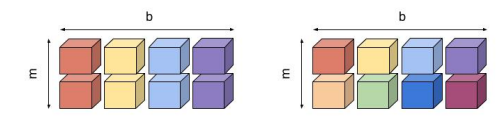


**Figure 1.** Shards of a 3-dim. tensor on a 2-dim. mesh (axes b and m). Blocks correspond to different devices, colors correspond to different shards (i.e. different data). Left: sharding along axis b. Right: sharding along axes b and m.

In this paper, we address the challenge of automatically expanding the search space to include interesting sharding strategies for intermediate tensors, without making this space intractably large. Our contributions are as follows:

- A novel static analysis that operates ahead of the partitioning search to identify tensor dimensions that must be sharded identically.
- A method for identifying and leveraging *sharding conflicts*—situations where an operation's sharding is ambiguous based on its operands. We demonstrate that these conflicts precisely define the search space for beneficial internal resharding strategies (Section 3.3).
- The other auto-sharding tool (TOAST). An automatic partitioning tool that integrates our analysis with a Monte-Carlo Tree Search agent [6]. The analysis guides the agent by (1) augmenting the search space with *conflict resolution actions* and (2) pruning the space by identifying dimensions that must be sharded together. This design enables the efficient discovery of complex resharding strategies (Section 4).
- A comprehensive evaluation (Section 5) demonstrating that TOAST consistently outperforms state-of-the-art automated and expert partitioning strategies across various ML models and hardware platforms.

#### 2 Background

#### 2.1 Partitioning of ML models

In the context of ML models, it is a common abstraction to organize the available accelerator devices (e.g. GPUs, TPUs) into a (logical) mesh, i.e. into an n-dimensional lattice that is spanned by n device axes (cf. [2, 22, 37, 45]). In this section, we assume that devices are organized in a 2-dim. mesh, spanned by axes b and m. If there are b devices along axis b and m devices along m, then the whole mesh consists of  $b \cdot m$  devices.

Partitioning an ML model is the process of preparing it for execution on a mesh of devices. This process involves distributing the model's tensors across the devices as smaller chunks, *shards*. A shard is created by slicing a tensor along one of its dimensions and assigning it to devices along a corresponding axis of the device mesh, as illustrated in Figure 1.

To illustrate these concepts, we look at the simplified MLP (*multi-layer perceptron*) in Figure 2a. There are two matrix multiplications, and a non-linear operation (ReLU) in

between. The inputs, or *samples*, are passed in as x, and the model parameters are given as arguments w1, w2.

We observe that all operations in the body of mlp act as maps across the tensor dimensions highlighted in yellow: 256. Thus, all operations can be executed in parallel on shards of tensors along these dimensions. Figure 2b uses the annotation {b} to indicate that these dimensions have been sharded along axis b. Although the body of mlp appears unchanged, its operations now execute on smaller tensors, specifically the shards corresponding to the full tensors shown in Figure 2a. Figure 2b is the batch-partitioned version of the mlp function. The function now operates on a shard of the input samples x, known as a batch. This listing shows the device-local code for mlp, where each device initially holds one such shard of x. During execution, each device computes shards of intermediate tensors. Consequently, the returned tensor w on each device represents a shard of the full output tensor from Figure 2a. Our batch partitioning of mlp requires no communication between devices.

Generally, partitioning relies on cross-device communication to ensure that the distributed execution of a model yields results identical to the results computed by the unpartitioned model. MPI-style primitives are typically used for collective communication between devices in the mesh [40]. Next, we develop an example of this. The mlp function in Figure 2b can be further partitioned. For example, partitioning the yellow dimension (256) along additional device axes, leading to smaller batches being processed by each device. But note how the parameters w1 and w2 did not get partitioned this way, even though we may want to to shard them to fit memory constraints. To achieve this, observe that the first matmul and the ReLU operations act as maps across the dimensions highlighted in green (64). Hence, sharding these dimensions again leads to independent device-local computations, up to the definition of z. In the final matmul, however, the green dimension is reduced over. If each device operates on a shard of z (and a shard of w2), only a contribution to this reduction is computed locally. To sum up the contributions from the devices, all\_reduce-style communication is required after computing the device-local matmuls.

Figure 2c shows the device-local code for mlp after sharding the green dimensions along axis m (after batch partitioning along b). The final reduction is performed across axis m, indicated by the attribute {m} on the all\_reduce. This kind of partitioning model parameters that are used in pairs of matmuls is the essence of Megatron partitioning [38].

#### 2.2 Partitioning, algorithmically

We have demonstrated batch and Megatron partitioning strategies on our mlp example. Each strategy requires sharding a specific set of tensors along particular dimensions, corresponding to the colored dimensions in Figure 2a. In

```
def mlp(x : [256, 32],
                                           def mlp(x : [256{b}, 32],
                                                                                         def mlp(x : [256{b}, 32],
        w1 : [32, <mark>64</mark>],
                                                    w1 : [32, <mark>64</mark>],
                                                                                                  w1 : [32, 64{m})],
         w2 : [<mark>64</mark>, 16]) {
                                                     w2 : [64, 16]) {
                                                                                                  w2 : [(64{m}, 16]) {
                                             y : [256{b}, 64] = matmul(x, w1)
    : [<mark>256</mark>, <mark>64</mark>] = matmul(x, w1)
                                                                                          y : [256{b}, 64{m}] = matmul(x, w1)
     : [256, 64] = ReLU(y)
                                             z : [256{b}, 64] = ReLU(y)
                                                                                           z : [256{b}, 64{m}] = ReLU(y)
                                             w : [256\{b\}, \overline{16}] = matmul(z, w2)
    : [256, 16] = matmul(z, w2)
                                                                                           w_{-}: [256{b}, 16] = matmul(z, w2)
                                                                                           w : [256{b}, 16] = all\_reduce {m} w_
  return w
                                             return w
 (a) Simple ML model: two linear layers. (b) Batch partitioning along device axis {b}.
                                                                                                (c) Batch and model partitioning.
```

Figure 2. Two-layer MLP with annotations. We highlight dimensions that should be sharded the same way.

this manual approach, the correct dimensions were identified by inspecting the operations in the mlp with the goal of minimizing communication.

How can a tool discover the right sets of dimensions? Simply enumerating all possible partitionings for all tensors does not scale with the ML model size. Hence the need for a systematic method to focus on candidates for partitionings.

How it was done before. Tools like Automap [3, 36], rely on compiler-based propagation of tensor shardings found in partitioning engines [2, 28, 45]. E.g. in the mlp function above, a search agent would only issue a sharding of the 64-sized (green) dimension of w1. The compiler would propagate this sharding to partition the first matmul, then through the ReLU, reach the second matmul, and finally propagate the sharding to the other parameter w2, and emit an all-reduce. Alpa [47] encodes the sharding as a logical mapping of dimensions to sets of devices, and employs internal propagation-like heuristics to simplify these constraints.

*Enter named dimensions.* If we had a way to identify, ahead of partitioning time, the dimensions that should be sharded together – i.e. dimensions with the same color in Figure 2a – then partitioning becomes simpler: pick an axis a and a color C, and shard all tensors whose dimensions include C along the dimension colored with C. This is the idea we build on for the rest of the paper.

The static analysis we present in Section 3 discovers sets of dimensions analogous to the colored dimensions in Figure 2a by carefully identifying *logical dimension names* based on rules that describe the parallel and contracting dimensions for every operation. These sets of dimensions act as the search space for our automatic partitioner (Section 4).

Named dimensions for resolving sharding conflicts. Beyond the apparent simplicity, our analysis is able to identify, ahead of time, situations where different dataflow paths originating from the same tensor lead to sharding ambiguities. Function f below provides an example: x flows into the matmul along two dataflow paths, directly and through y.

```
def f(x : [32, 4]) {
  y : [4, 32] = transpose(x)
  z : [32, 32] = matmul(x, y)
```

```
return z
}
```

Propagating the sharding of x along both paths leads to an ambiguity for sharding the matmul. For example, if x is sharded on its first dimension (of size 32), then y is sharded on the second dimension, and it is now unclear whether matmul should become sharded along its first or second dimension. Conceptually, if we were to assign colors to dimensions, matmul would receive the same color on both dimensions, a situation that we call a sharding conflict. When partitioning the matmul operation along that color, we need to pick which one of the two dimensions of that color to shard.

Our analysis is not only able to discover these ambiguities but – going further – we show that by keeping track of different dimension names for different uses of tensors we are able to extract all the possible choices for resolving these sharding conflicts (Section 3.3), and later surface them as part of the search space (in MCTS). This ability is key to enabling TOAST to partition attention computations [44], the cornerstone of modern Large Language Models, at context lengths beyond what other methods are capable of.

#### 3 Named Dimension Analysis

We now describe our static analysis that discovers sets of dimensions analogous to the colored dimensions in Figure 2a. Each op in the program is assigned unique dimensions for its operands and its results, some of which we identify (unify) by inspecting a rule that tells us how the dimensions of operands or results can be sharded together. For example, a matmul can be computed in a sharded fashion along its first dimension if provided with shards of its first operand also on the first dimension. The rules are populated ahead of time for every op in our array IR, analogously to [2, 28].

After identifying dimension names based on all the rules that apply to the operations in a program, each remaining (unidentified) dimension name will appear in a set of dimensions analogous to the colored dimensions in Figure 2a.

#### Tensor expressions in ANF **Auxiliary definitions** variable M ::= $\emptyset \mid \mathcal{M} \cup \{c \mapsto d\}$ ::= x $a, b, c, d, d_1, \ldots, d_k$ dimension names Map let $x = op(\overline{x})$ in elocal definition Named dimensions $\ \ I$ $\emptyset \mid I \cup \{d \stackrel{\circ}{=} c\}$ Identities $\overline{d} ::= [] \mid [d_1, \ldots, d_k]$ Environment $\cdot \mid E, x : \overline{d}$ $op \in \{f, add, transpose, matmul, ...\}$

#### Named Dimensions Analysis

 $NDA_{E:Environment}: (e:Expression) \rightarrow (\overline{d}:Named dimensions) \times (\mathcal{M}:Map) \times (\mathcal{I}:Identities)$ 

```
NDA_E(\text{let } x = op(\overline{x}) \text{ in } e)
                                                             (\overline{d}_2, \mathcal{M}_1 \cup \mathcal{M}_2, I_1 \cup I_2),
                                                                                                                                                             NDA_E(x)
                                                                                                                                                                                                       (\overline{a}, \{d_i \mapsto a_i\}, \emptyset),
(LET)
                                                             where (\overline{d}_1, \mathcal{M}_1, I_1) = NDA_E(op(\overline{x})),
                                                                                                                                                             (VARIABLE USE)
                                                                                                                                                                                                       if x : \overline{d} \in E, with a_i fresh
                                                                         (\overline{d}_2, \mathcal{M}_2, \mathcal{I}_2) = NDA_{E,x:\overline{d}_1}(e)
                                                                                                                                                             NDA_E(f(x))
                                                                                                                                                                                                       (\overline{a}, \mathcal{M}, \{a_i \stackrel{\circ}{=} d_i\}),
                                                             ([a_1,\ldots,a_{r-1},a_{r+1},\ldots,a_k],\mathcal{M},\{a_i\stackrel{a}{=}d_i\}),
                                                                                                                                                             (FUNCTION)
                                                                                                                                                                                                       where (\overline{d}, \mathcal{M}, \emptyset) = NDA_E(x),
NDA_E(reduce_{r,op}(x))
                                                                                                                                                                                                       with a_i fresh
(REDUCE)
                                                             where ([d_1, \ldots, d_r, \ldots, d_k], \mathcal{M}, \emptyset) = NDA_E(x),
                                                             with a_i fresh, for op \in \{add, mul, ...\}
                                                                                                                                                                                                       (\overline{a}, \mathcal{M}_1 \cup \mathcal{M}_2, \{a_i \stackrel{\circ}{=} d_i, a_i \stackrel{\circ}{=} c_i\})
                                                                                                                                                             NDA_E(op(x, y))
                                                             ([a_1, a_2], \mathcal{M}_1 \cup \mathcal{M}_2, \{a_1 \stackrel{\circ}{=} d_1, a_2 \stackrel{\circ}{=} c_2, d_2 \stackrel{\circ}{=} c_1\}),
                                                                                                                                                                                                       where ([d_1,\ldots,d_k],\mathcal{M}_1,\emptyset) = \mathsf{NDA}_E(x),
\mathsf{NDA}_E(\mathsf{matmul}(x,y))
                                                                                                                                                                                                                   ([c_1,\ldots,c_k],\mathcal{M}_2,\emptyset) = \mathsf{NDA}_E(y),
                                                             where ([d_1, d_2], \mathcal{M}_1, \emptyset) = NDA_E(x),
(MATMUL)
                                                                                                                                                                                                       with a_i fresh, for op \in \{add, mul, ...\}
                                                                         ([c_1, c_2], \mathcal{M}_2, \emptyset) = NDA_E(y), with a_1, a_2 fresh
                                                             ([a_1,...,a_r,...,a_l,...,a_k], \mathcal{M}, \{a_i \stackrel{\circ}{=} d_i\}),
\mathsf{NDA}_E(\mathsf{transpose}_{lr}(x))
                                                             where ([d_1, \ldots, d_l, \ldots, d_r, \ldots, d_k], \mathcal{M}, \emptyset) = NDA_E(x), with a_i fresh
(TRANSPOSE)
NDA_E(broadcast_i(x))
                                                             ([a_1,\ldots,a_{l-1},a,a_l,\ldots,a_k],\mathcal{M},\{a_1 \stackrel{\circ}{=} d_1,\ldots,a_{l-1} \stackrel{\circ}{=} d_{l-1},a_l \stackrel{\circ}{=} d_l,\ldots,a_k \stackrel{\circ}{=} d_k\})
(BROADCAST)
                                                             where ([d_1,\ldots,d_{l-1},d_l,\ldots,d_k],\emptyset,\mathcal{M}) = NDA_E(x), with a_i,\ldots,a_{l-1},a,a_l,\ldots,a_k fresh
```

**Figure 3.** The named dimensions analysis (NDA), illustrating the cases for several ops

#### 3.1 Definition of the analysis

Figure 3 defines our *named dimensions analysis* (NDA) as a recursive function that operates on straight line tensor programs in A-normal form [34], which is equivalent to the SSA form used in our implementation. Given an environment E that maps free variables to dimension names, the NDA computes a triple consisting of:

- (i) an assignment of dimension names to tensor op results,
- (ii) a mapping  ${\cal M}$  connecting dimension names of value definitions to the dimension names of their uses, and
- (iii) a set of identities  $\mathcal{I}$  between dimension names.

The dimension names assigned in (i) are the  $a_i$  that appear in Figure 3. To illustrate (i) and (ii), consider the following definition and use of variable y, assuming x is assigned dimension names  $[d_1, d_2]$  in the current environment E.

let 
$$y = x$$
 in  $y$ 

The LET rule in Figure 3 invokes the Variable use rule to determine that the use of x should be assigned fresh names  $[a_1,a_2]$  and the map  $\mathcal{M}$  should be populated with  $\{d_1 \mapsto a_1,d_2 \mapsto a_2\}$ . The LET rule then adds the assignment  $y:[a_1,a_2]$  to E, before invoking the Variable use rule again, this time for the use of y after in. The use of y is assigned fresh names  $[b_1,b_2]$ , and  $\mathcal{M}$  is extended with  $\{a_1 \mapsto b_1,a_2 \mapsto b_2\}$ . Notice how  $\mathcal{M}$  connects dimension names between definitions and uses:  $b_1$  and  $b_2$  from the use

of y can be traced all the way back to  $d_1$  and  $d_2$  from the definition of x.

The identities I from (iii) record which dimensions that appear in an operation should be sharded identically. We consider matmul(x, y) to illustrate this. Assuming that the the matmul rule in Figure 3 has assigned dimension names  $[d_1, d_2]$  and  $[c_1, c_2]$  to the use of x and y, respectively, we compactly express this instance of the matmul rule as

$$\mathsf{matmul}(x:[d_1,d_2],y:[c_1,c_2]):[a_1,a_2],$$

together with identities

$$a_1 \stackrel{\circ}{=} d_1$$
,  $a_2 \stackrel{\circ}{=} c_2$ ,  $d_2 \stackrel{\circ}{=} c_1$ .

The first identity expresses that matmul acts as a map on the leading dimension of the first operand, which means that if the first operand is sharded on that dimension, we can compute the matmul in a sharded way, and concatenate the shards on the leading dimension of the result to obtain the original result. The second identity is analogous. The third one expresses that we can shard the matmul by sharding both operands along the contracting dimension. (Lowering must then introduce an all\_reduce, as in Figure 2c.)

#### 3.2 Partitioning functions with the NDA

Figure 4a shows the mlp function from Figure 2a annotated with the results computed by the NDA. Tensor variables, and their uses, are annotated with named dimensions (not with actual shapes). The map  ${\cal M}$  and the identities  ${\cal I}$  computed by the NDA appear in comments.

In going to Figure 4b, we have applied the identities from I. This reveals the different ways in which each operation in the function body can be partitioned, in isolation, as explained in Section 3.1. In comments, we still display the map  $\mathcal{M}$ , but the identities from I have also been applied to  $\mathcal{M}$ . Note that the entries of  $\mathcal{M}$  still point from dimension names in the definitions of variables (including function arguments) to the dimension names in variable uses.

To connect the partitionings of individual operations in a function body, we consider the entries of  $\mathcal M$  as identities, and apply them to further identify dimension names. This leads to Figure 4c. Where B corresponds to the yellow, and U to the green colors of Figure 2a.

In conclusion, identifying the dimension names (assigned by the NDA) with identities from  $\mathcal{I}$  and  $\mathcal{M}$  (also computed by the NDA) produces sets of dimensions like the ones we found manually in Section 2.1. Sharding these sets of dimensions along device axes leads to partitionings of whole functions.

#### 3.3 Sharding conflicts

While identifying dimension names with both I and M leads to the desired sets of dimensions for sharding, it may also introduce a problematic ambiguity: the same dimension name may appear more than once among the names that annotate the same variable, as for tensor z below.

```
def f(x: [S, T]) {
   y : [T, S] = transpose(x: [S, T])
   z : [S, S] = matmul(x: [S, T], y: [T, S])
   return z
}
```

When attempting to shard all dimensions that are labeled S, which of the dimensions of z should be sharded? One axis cannot shard more than one dimension of a single tensor.

When the same dimension name occurs more than once among the names assigned to a tensor, we refer to this as a *sharding conflict* (or just *conflict*). Conflicts prominently occur in the attention layer of the Transformer model [44]. Figure 5a shows a simplified self-attention computation from the Transformer architecture, annotated with dimension names after identifying with I and M. Up to the definition of a, the attention computation is standard. Notice that a has a conflict since S occurs twice in its annotation.

To ease the presentation, Figure 5a replaces the softmax computation in standard attention with an averaging computation, which (like softmax) includes a reduction and pointwise operation. Note that the reduce makes the conflict from a disappear, since it removes the reduced-over dimension. Conflicts appear again in the results of broadcast and div: the op rule in Figure 3 forces the conflict from a also onto c and d. Lastly, the final matmul contracts over dimension S and thus removes the conflict present in d.

When sharding a set of dimensions that are labeled with the same dimension name, conflicts may generally need to be resolved. That is, for each tensor where the dimension name appears more than once, one must choose one of the dimensions for sharding. In Figure 5b, the conflicts in the attention layer have been resolved by sharding the last dimensions of a, c and d along axis s, introducing an all\_gather and a reduce\_scatter operation. This partitioning of the attn function is known as sequence sharding [20] and is required for scaling the Transformer sequence length.

#### 3.4 Sharding in the presence of conflicts

Because of the possibility of conflicts, we cannot simply shard all dimensions that have been assigned the same name by the NDA (after identifying names with I and I). We must additionally specify how conflicts should be resolved if they occur. Instead of defining another analysis that discovers conflicts and offers resolutions, we can in fact re-use the NDA to produce also conflict resolutions. The key idea here is:

Do not identify dimension names with the definition-to-use map  $\mathcal{M}$ , but only using the sharding rules identities  $\mathcal{I}$ .

To illustrate this idea, we show the simplified attention layer from Figure 5a again in Figure 5c, this time identifying dimension names only with the identities in I. As we have seen before, this means that each operation is annotated with fresh dimension names, and each name corresponds to precisely one way in which an operation can be partitioned. Instead of listing the entries of the map  $\mathcal{M}$ , a fraction of  $\mathcal{M}$  is pictured as a graph in Figure 5d: each black, directed edge corresponds to an entry in  $\mathcal{M}$ . When we think of the full map  $\mathcal{M}$  as a graph, we refer to this as the *dimension graph*, since the nodes in this graph are dimension names. The fraction of the dimension graph in Figure 5d is the connected component of S. This is the only connected component of  $\mathcal{M}$  whose dimension names participate in conflicts.

When not identifying dimension names with  $\mathcal{M}$ , we must characterize conflicts differently from before: a conflict occurs between any pair of dimension names that annotate the same variable definition or use. Conflicts in the attn function are drawn as red, undirected edges in Figure 5d. Three of the five conflicts are precisely the conflicts in variables a, c and d that we saw in Figure 5a already. The additional two conflicts come from the uses of c and d, respectively.

Each conflict edge can be resolved in two ways, picking one or the other endpoint – a total of 32 resolutions. Unfortunately, 32 resolutions for just sharding the sequence length of a transformer significantly increases the search space for automation. Next, we discuss two heuristics for reducing the number of conflicts that need independent resolutions.

#### 3.5 Compatible conflicts

Conflicts in variable definitions and the corresponding variable uses should be attempted to be resolved in the same way, if we wish to avoid communication (resharding). Consider

```
def mlp(x : [B, X], w1 : [T, U], w2 : [V, W]) {
                                                                    def mlp(x : [B, X], w1 : [T, U], w2 : [V, W]) {
  y : [A1, A2] = matmul(x : [B1, X1],
                                                                      y : [A1, A2] = matmul(x : [A1, X1],
                                 w1 : [T1, U1])
                                                                                                     w1 : [X1, A2])
      # from use of x: B \rightarrow B1, X \rightarrow X1
                                                                           \# B -> A1, X -> X1, T -> X1, U -> A2
      # from use of w1: T \rightarrow T1, U \rightarrow U1
                                                                          : [C1, C2] = ReLU(y : [C1, C2])
      # from matmul: A1 \stackrel{\circ}{=} B1, A2 \stackrel{\circ}{=} U1, X1 \stackrel{\circ}{=} T1
                                                                           # A1 -> C1, A2 -> C2
     : [C1, C2] = ReLU(y : [D1, D2])
                                                                          : [E1, E2] = matmul(z : [E1, V1],
      # from use of y: A1 \rightarrow D1, A2 \rightarrow D2
                                                                                                     w2 : [V1, E2])
      # from ReLU: C1 \(^2\) D1, C2 \(^2\) D2
                                                                           # C1 -> E1, C2 -> V1, V -> V1, W -> E2
     : [E1, E2] = matmul(z : [F1, F2],
                                                                       return w
                                w2 : [V1, W1])
                                                                    }
      # from use of z: C1 \rightarrow F1, C2 \rightarrow F2
                                                                               (b) Dimension names identified with I only
      # from use of w2: V \rightarrow V1, W \rightarrow W1
      # from matmul: E1 \stackrel{\circ}{=} F1, E2 \stackrel{\circ}{=} W1, F2 \stackrel{\circ}{=} V1
                                                                    def mlp(x : [B, X], w1 : [X, U], w2 : [U, W]) {
  return w
                                                                         : [B, U] = matmul(x : [B, X], w1 : [X, U])
}
                                                                          : [B, U] = ReLU(y : [B, U])
                                                                          : [B, W] = matmul(z : [B, U], w2 : [U, W])
         (a) NDA results, entries of \mathcal{M} and \mathcal{I} in comments
                                                                       return w
                                                                    }
```

**Figure 4.** Application of the NDA to the two-layer MLP from Figure 2

a fragment of a dimension graph that looks like the "box" on the left of Figure 6: N and O are dimension names in the definition of a variable, and L and R are names in a use of the same variable. If the two conflicts are resolved differently, say N was sharded (but not O) and R was sharded (but not L), resharding with an all\_to\_all communication primitive [40] is required between variable definition and use. On the other hand, if N and L are both sharded, no resharding (and hence no communication) is needed.

We refer to pairs of conflicts as *compatible* if, in the dimension graph, they form a "box" (Figure 6, left). In real ML models, more complex dataflow may complicate matters: there may also be paths in the dimension graph going across the "box" (Figure 6, middle and right). If such paths exists, we do not deem conflicts compatible.

Motivated by avoiding extra communication while reducing the number of independent resolutions, we decree that compatible conflicts should be resolved in the same way. We construct sets of compatible conflicts by considering the reflexive, symmetric and transitive closure of the compatibility relation, which we refer to as *compatibility sets*. In Figure 5d there is only one compatibility set, containing all conflicts: {(S111, S311), (S111, S31111), (Sc, S31111), (Sc1, S3112), (Sc11, S21)}. There are two resolutions, one of which leads to the sequence sharding from Figure 5b. The other introduces two all\_gathers and has different memory and runtime characteristics; we omit it for lack of space.

#### 3.6 Conflict compatibility across layers

(c) Dimension names identified with I and M

Our second heuristic identifies compatibility sets of conflicts that originate from repeated layers in ML models. Each compatibility set C can be thought of as a sub-graph of the full dimension graph, containing just the nodes C and any edges with endpoints in C. For repeated layers, these graphs are necessarily isomorphic. When compatibility sets  $C_1$ ,  $C_2$  are isomorphic, we decree that corresponding pairs of conflicts from  $C_1$  and  $C_2$  should be resolved in the same way.

For Transformers, this heuristic successfully identifies all (forward) attention layer compatibility sets, and also all corresponding compatibility sets in the backwards layers. Since each forward and backward layer has one compatibility set, we only get 4 different conflict resolutions for the Transformer architecture, regardless of the number of layers.

### 4 TOAST: The other auto-sharding tool

The NDA exposes sets of tensor dimensions that should be sharded identically. Importantly, it identifies conflict compatibility sets. We now describe TOAST, a system built to leverage the NDA into an automatic partitioner, via a simulated cost model for runtime and memory estimation interpreting device-local IR we generate. For reference, Figure 7 tracks the various components of TOAST. It is frontend (i.e., JAX [5], PyTorch [30]) and backend (e.g., XLA[10]) agnostic. It operates over an array IR – StableHLO [21, 29], that frontends frequently lower to, and backend compilers and runtime systems can ingest and execute on a variety of hardware

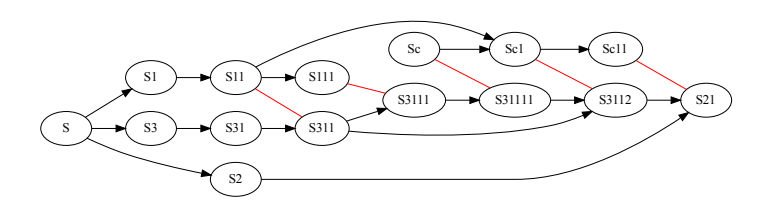
<sup>&</sup>lt;sup>1</sup>We omit the detailed example for reasons of space.

```
def attn(x : [S, D] , wq : [D, H1],
          wk : [D, H1], wv : [D, H2]) {
  k : [S, H1] = matmul(x, wk)
  v : [S, H2] = matmul(x, wv)
                                  # values
  q : [S, H1] = matmul(x, wq)
                                  # gueries
  qt: [H1, S] = transpose(q)
  a : [S, S] = matmul(k, qt)
  # begin: mock softmax computation (averaging)
               = reduce<sub>1,add</sub>(a)
  b : [S]
      [S, S] = broadcast_0(b)
  d:[S, S] = div(a, c)
  # end: mock softmax computation (averaging)
  z : [S, H2] = matmul(d, v)
  return z
}
```

(a) Named dimensions, identified with I and M

```
def attn(x : [S{s}, D], wq : [D, H1],
         wk : [D, H1] , wv : [D, H2]) {
  k : [S{s}, H1] = matmul(x, wk)
  v : [S{s}, H2] = matmul(x, wv)
  q : [S{s}, H1] = matmul(x, wq)
  qt: [H1, S{s}] = transpose(q)
  k_: [S, H1]
                  = all_gather {s} k
  a : [S, S{s}] = matmul(k_, qt)
                  = reduce<sub>1,add</sub>(a)
  b : [S{s}]
                = broadcast<sub>0</sub>(b)
  c : [S, S{s}]
  d : [S, S\{s\}] = div(a, c)
  z_: [S, H2]
                  = matmul(d, v)
  z : [S{s}, H2] = reduce\_scatter {s} z_
}
```

(c) NDA results, after identifying with I only



**(d)** Dimension graph (component connected of S): nodes refer to dimension names in listing (c) above; conflicts shown as undirected edges (in red)

(b) One possible resolution for sequence sharding

**Figure 5.** Simplified attention computation (mocking-up softmax as averaging for illustration purposes)

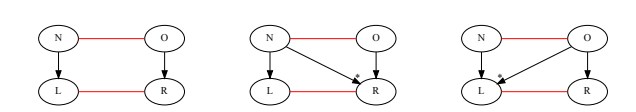


**Figure 6.** "Box" of compatible conflicts (left) and incompatible conflicts, with paths going "across" (middle and right).

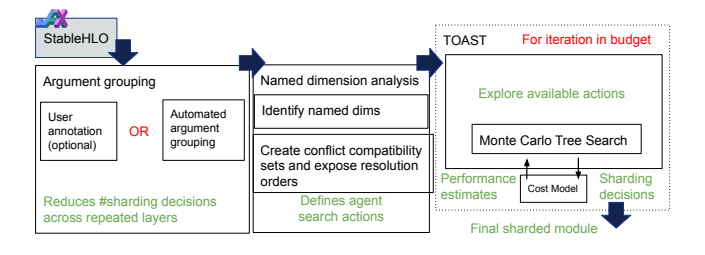


Figure 7. TOAST overall system architecture.

platforms. The TOAST partitioner is built as a Monte-Carlo Tree Search (MCTS) [6].

#### 4.1 MCTS: background

The goal of TOAST is to find and apply sequences of actions that progressively shard an ML model. The core components are: (1) the state s of the search; (2) the reward model R(s) (Section 4.5) that assigns values to states, showing relative improvement (or deterioration) in expected performance; (3) a set of actions that can be taken from a state s.

MCTS has been used successfully in many domains, including games, systems, and partitioning [3, 4, 25, 36, 39]. The algorithm balances exploration (gaining new information about possible action sequences) with exploitation (leveraging previously identified high-performing actions). Our implementation is multi-threaded, generating many trajectories, sequences of actions paired with their estimated performance, in parallel. A single round of MCTS consists of unrolling all trajectories and identifying the best-performing

one to apply to the target module. Our method adapts a standard MCTS framework with several key heuristics tailored to our problem. First, while MCTS is typically run for a fixed computational budget, we terminate the entire search process early if a round of new trajectories fails to improve upon the best-known cost. Second, within the search, we weigh the MCTS actions to incentivize shorter trajectories. Early termination of individual rollouts is crucial because our system, NDA, shards multiple dimensions simultaneously; shorter trajectories enable a more precise credit assignment, helping to better isolate and estimate the performance impact of sharding a specific dimension.

#### 4.2 Axis-aware and color-based actions

Based on a model's NDA and its compatibility sets (Figure 5d), we design the available actions as tuples of the form:

dim\_name × resolution\_order × axis

When an action is applied, the agent attempts to shard all dimensions corresponding to the dim\_name onto the set of devices belonging to axis. The resolution\_order is a bitstring to resolve the sharding conflicts that may arise. Since each compatibility set offers two possible resolutions, a model with b such sets requires a b-bit string for the resolution\_order, where the i-th bit selects the resolution for the i-th set. In TOAST, we pre-compute these compatibility sets at the construction time. During the MCTS search, the agent's chosen action tuple determines which of the pre-calculated resolutions to apply. Each dim\_name is encoded as a unique identifier, which we refer to as a *color*.

The MCTS search begins with a one-time setup where the initial action space is constructed from all possible triplets for the module. We prune this space by discarding actions affecting fewer than 10 unique dimensions, as these trivial operations do not meaningfully improve performance. The search then proceeds by simulating numerous trajectories from the game tree's root (unsharded module). Each trajectory simulation is a sequence of the following steps:

- 1. An action is selected from the current state's set of available actions based on the MCTS selection policy.
- 2. The simulation state is updated. This involves removing the action just taken from the available set, as well as pruning any other actions that have become invalid as a consequence of the new sharding state.
- 3. The simulation of the trajectory ends, or reaches a terminal state, if one of the following conditions is met: (a) a special *stop* action is selected, or (b) a maximum trajectory depth is reached (which we set to 30 actions).

This process of simulating trajectories is repeated until the global computational budget is exhausted, at which point the best-found action sequence is returned.

#### 4.3 Colors aware state

A key component of MCTS is the state representation, which must uniquely and efficiently identify each node in the search tree and its expected performance. A naive approach of tracking the sequence of applied actions is insufficient, as different action orderings can result in the same sharded model, leading to duplicated states and exponentially expands the amount of evaluation needed to explore the space. Another alternative, serializing the entire module after each action, while it is guaranteed to not introduce duplicates, is computationally prohibitive. A more recent approach [3] tracks the sharding state of the function's arguments. However, this method cannot distinguish between different sharding configurations of intermediate tensors (i.e., tensors that are not function arguments). This ambiguity introduces a drawback where multiple distinct actions lead to the same state representation, necessitating complex, retrospective pruning mechanisms like level 2 action transposition [7].

To overcome these limitations, we leverage NDA to define our state. Our representation is an efficient in-memory map that records the sharding configuration of every dimension in the module. This design provides several key advantages:

- Efficient: It avoids the cost of serializing the module by only tracking the dimensions that have been sharded.
- Unambiguous: The state is defined by the final sharding configuration itself, not the sequence of actions taken. Consequently, any action sequence yielding the same sharded model resolves to the same unique state, eliminating duplication by construction.
- **Simple**: By computing the action space ahead of time and exposing only unique, canonical actions, we eliminate the possibility of redundant actions in the search space. This proactive design avoids the need for complex run-time pruning mechanisms entirely.

#### 4.4 Grouping repeated layers

The repeated layers common in modern ML models, each containing its own set of parameters, cause the decision space for auto-sharding to grow exponentially. Sharding conflicts introduce another layer of exponential complexity. While our heuristics (Sections 3.5 and 3.6) address the latter by reducing the number of independent resolutions, they do not solve the initial problem. Specifically, they do not identify opportunities to apply consistent sharding decisions across these repeated layers.

To address this challenge, Alpa [47] discovers groups of sharding decisions that should be made consistently across model layers by timing and memory live range analysis. TOAST, on the other hand, uses a structural heuristic: we group function arguments based on keys constructed from all uses of the (dimension names of) these arguments. The intuition is that repeated layers use function arguments that

correspond to model parameters similarly. Whenever an action is applied to a dimension, it is mirrored to the corresponding dimensions of all grouped arguments.

#### 4.5 Cost model

MCTS requires a way to evaluate the impact of a sequence of actions on a partitioned ML model. We rely on a fast and approximate cost model that involves analytical and roofline calculations to estimate compute op runtime as well as communication runtime for collectives (e.g. all\_gather, all\_to\_all, all\_reduce etc). The cost model takes into account the device's characteristics, such as its FLOPS and network characteristics. The cost model is derived from an abstract interpreter of the MLIR module, where runtime cost is accumulated along the critical path. We take into account only matrix-multiplication ops (e.g. dot\_general, convolution) and we provide cost estimates for different choices of collective implementation. We finally perform a live range analysis to approximate peak memory usage.

Instead of absolute cost, MCTS only needs to know the *relative improvement* between states. For example, we would expect batch partitioning across b devices to reduce runtime by a factor of b. Therefore, we define the cost of state s as C(s) = RT(s) + MP(s), where RT(s) and MP(s) are *relative* runtime (RT) and memory penalty (MP), respectively:

$$RT(s) = \frac{\text{current runtime}}{\text{initial runtime}}$$

$$MP(s) = C \cdot \frac{\text{current peak} - DM}{\text{initial peak memory}} \cdot \begin{cases} 1, & \text{if current peak} > DM \\ 0, & \text{otherwise} \end{cases}$$

*DM* is the available amount of per-device memory. So *MP* penalizes a state *s* only if the partitioned module's memory requirements (current peak) exceed the amount of local, per-device memory. The constant *C* controls how much of a penalty is incurred for exceeding memory constraints.

#### 5 Evaluation

We evaluate TOAST on two criteria: (1) its ability to discover partitioning strategies that outperform expert-designed and related state-of-the-art (SOTA) methods across diverse hardware and model architectures (Section 5.2), and (2) its lower overhead compared to competing methods (Section 5.3).

#### 5.1 The setup

We partition a range of popular models used in competition [24]. These models are written in JAX [5], trained with Adam [19], and compiled with XLA [10]. We turned off XLA's rematerialization to avoid noisy measurements:

**T2B/T7B** the 2B and 7B Gemma1 Transformer models [42]:

	$d_{model}$	layers	hidden dim.	heads	key size	vocab.
T2B	2048	18	32768	8	256	256128
T7B	3072	28	49152	16	256	256128

**GNS** a 875M-parameters graph neural network used to simulate physical systems [9, 35]. Graphs contain 2048 nodes and

8192-65536 edges, mimicking a molecular structure. We perform 24 message-passing steps over 3 linear layers (hidden size: 1024; latent size: 2048).

**U-Net** a 3.6B-parameters convolutioned neural network, popular in medical imaging [14, 33] and diffusion models [12]. We use 9 residual down-sampling blocks, 12 up-sampling blocks, and between them a 32-head attention layer.

ITX a 5B-parameters inference optimized transformer [31], featuring ROPE [41] and a KV cache [31]. (Vocab. size: 50257; sequence length: 1024; prompt length: 1024; 32 heads; 32 layers; hidden dim.: 4096; d\_model: 2048.)

We conducted the experiments on set of A100 [26] and P100 [27] GPUs and on TPUv3 [8], with NVidia's NVLINK and ICI [16] connectivity respectively. For the experiments, we partition the models with Alpa [47], AutoMap [3, 36], TOAST, and expert-driven (i.e. manual) annotations.

## **5.1.1 Expert/manual sharding.** For each model, we use an expert-designed *Manual* sharding strategy as our baseline, which we detail below:

- 1. **T2B**, **T7B**: We partition these Transformer models using a fully-sharded data parallel (FSDP) [32, 46] strategy, combined with Megatron-style [38] sharding of the MLP and attention-head layers, and sequence parallelism [20]. Our *Manual* baseline represents the best-performing configuration found after exhaustively searching all combinations of these strategies.
- 2. **GNS**: The SOTA strategy is edge sharding [11]. However, we found that combining this with Megatronstyle [38] partitioning of the linear layers within each node and edge processor of the GNS improves both runtime and memory performance.
- 3. **U-Net**: The industry-known *manual* strategy combines FSDP [46] with Megatron-style partitioning [38].
- 4. ITX: For this inference-optimized Transformer model, the standard scaling approach combines multi-query attention sharding [31], Megatron partitioning [38], and data parallelism over the batch dimension.

Developing these manual strategies required significant expert effort to augment SOTA partitioning techniques with further sharding optimizations. The novelty and complexity of these approaches are evidenced by the multiple publications dedicated to them. We argue that TOAST, despite being model- and hardware-agnostic, is highly competitive with these specialized, heavily-researched strategies.

#### 5.2 Auto-sharding of a wide range of models

This set of experiments evaluates the generalizability of our automatic sharding tool across various models and hardware configurations. A key motivation is that manual sharding annotations are often brittle; when a pre-trained model is adapted to a new use case or deployed on different hardware, its original annotations can lead to sub-optimal performance. Revising these annotations is a complex, error-prone process

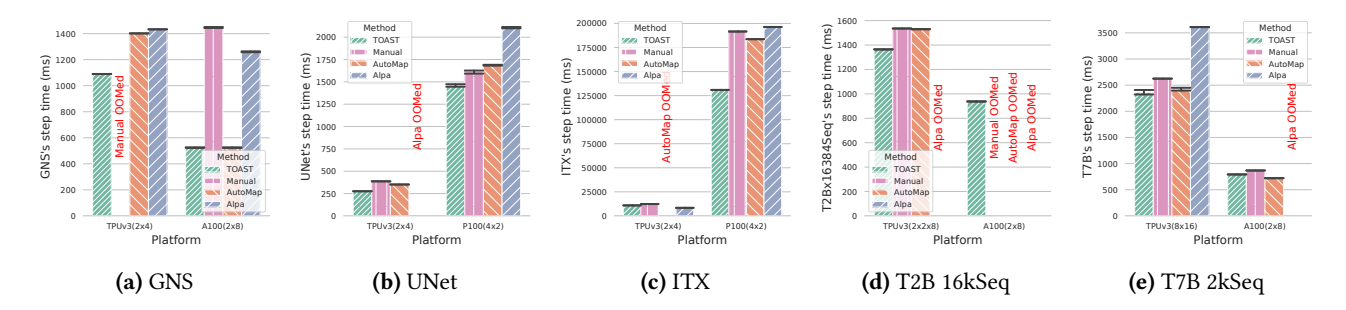


Figure 8. Partitioned model step time in milliseconds (lower is better).

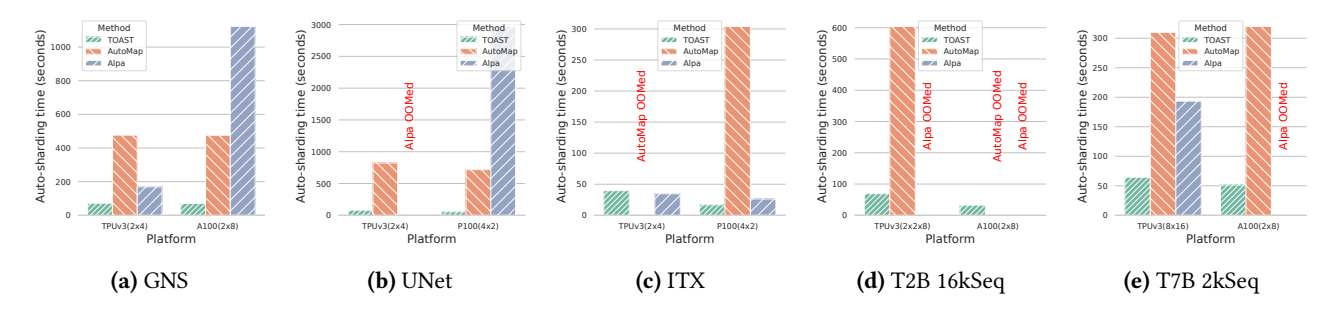


Figure 9. Auto-sharding search time in seconds for the partitioned solution (lower is better).

requiring significant expertise, which poses a substantial barrier to porting models effectively.

Figure 8 shows the *model step time*, the execution time for a single training or inference step—across all experiments, each repeated 10 times for hundreds of steps. Across all tested models and hardware configurations, TOAST consistently finds better partitioning strategies than the baselines. Notably, in cases where baselines do not cause an out-ofmemory error (OOM), the step times of heavily optimized manual strategies on TPUs, where they are battle-tested, are very close to those discovered by TOAST. While Alpa and AutoMap have a cost model that penalizes solutions that exceed available on-device memory similar to TOAST, in some scenarios (such as the 16k sequence length T2B experiment on GPU) they are not able to avoid OOMs, while TOAST is able to do so. The action tuples available to TOAST (Section 4.2) provide important trade-offs related to the order of conflict resolution, a key contribution of this paper which is unavailable to other automatic tools. By resolving conflicts in a specific order, TOAST can reduce the peak memory usage of the partitioned model. This memory optimization is critical, as it can enable partitioning strategies with lower step times that would otherwise be infeasible due to memory constraints. We want to stress that even a 1% improvement in step time translates to weeks of saved computation, given that a model is compiled once with TOAST but then trained or served for months at a time [13].

Another key result is that TOAST consistently finds a superior sharding strategy across diverse hardware configurations, a crucial capability for enabling hardware fungibility at scale. Furthermore, TOAST's performance reveals that many model architectures are under-optimized. For instance, while its results on well-studied Transformer models are comparable to heavily tuned *manual* strategies, it discovers significant improvements for other architectures. This finding suggests that standard industry techniques, such as the one used for GNS, are often suboptimal.

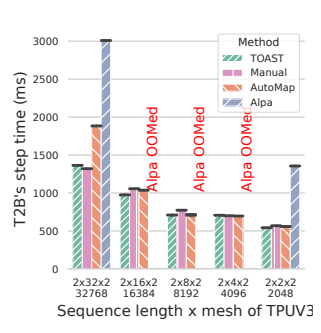
#### 5.3 Auto-sharding overhead

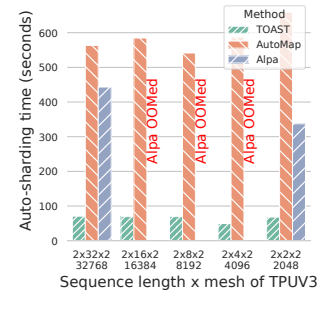
A key differentiator among auto-sharding methods is the time required to find sharding decisions. An auto-sharding tool with a tolerable search time is more likely to be adopted for interactive model development, unlike methods suitable only for a model's final production run. Figure 9 compares the search times for Alpa, AutoMap, and TOAST. We observe that Alpa, which is optimized for TPU workloads, is significantly slower on GPUs, while AutoMap and TOAST exhibit platform-agnostic runtimes. We suspect this performance discrepancy stems from assumptions embedded within its linear programming solver; its cost model constraints are tuned for TPUs and thus require significantly more evaluation to meet GPU constraints.

While AutoMap is consistent with its performance across platforms, it remains significantly slower than TOAST. AutoMap has to invoke the underlying propagation system after every action, which explains why, for complex models that

need many actions, its search time can be orders of magnitude slower (25× for UNet and GNS). In contrast, TOAST precomputes the propagations ahead-of-partitioning. When the MCTS agent selects an action, it performs a fast, in-memory mutation to record the choice of color and resolution order. These decisions are only materialized and applied to the module during cost model estimation. Furthermore, many of the NDA queries are heavily cached; once conflicts and their compatibility groups are computed, they are accessed in O(1) time during the conflict resolution phase. These design choices make TOAST's search time largely platformand model-size-agnostic.

#### 5.4 Scaling devices and sequence length





- **(a)** Step time in millisecond (lower is better).
- **(b)** Search time in seconds (lower is better) scaling with number of devices.

**Figure 10.** Partitioned T2B and scaling its sequence length and devices in a 3D mesh of 'BatchxSeqxModel', the number of devices can be calculated by multiplying the different axes size, e.g., 2x32x2 = 128 device for the 32k sequence length.

Finally, we evaluate the scalability of our sharding solution as the model's sequence length and the number of devices increase. A good sharding solution must stay within the memory constraints of the available hardware and achieve performance comparable to an expert-derived baseline. Scaling a Transformer's sequence length is particularly important, as it enables it to capture the long-range dependencies between tokens to solve complex real-world problems.

As shown in Figure 10, TOAST achieves near-optimal scaling, with performance comparable to expert-driven sharding strategies that required hundreds of engineering hours to develop. It outperforms SOTA methods like AutoMap by leveraging the novel conflict resolution and NDA to operate over intermediate values, as motivated earlier in this paper. In contrast, under the high memory pressure of these scaling experiments, Alpa frequently triggered OOM errors or failed to find optimal solutions.

#### 6 Related work

Partitioning systems like GSPMD [45], Shardy [28], and PartIR [2] rely on user manual sharding. They are effective at propagating the manual sharding on inputs, but require users to know where to place the manual shardings. Without a clear signal how far the propagation will go, users are left with trial and error as the main mechanism to discover good sharding decisions. Propagation based on PartIR and GSPMD may introduce conflicts, that need to be handled with sharding constraints in the case of GSPMD, and special tag ops in PartIR case. Discovering where to place these constraints requires often a lengthy iteration and profiling by experts. Our NDA and conflict resolution system identifies a small set of these conflicts ahead-of-time, and serializes their resolution in the action space. Fully-automatic partitioners such as Alpa[47], FlexFlow[15], Unity[43], and Galvatron[23] developed to simplify the task of sharding for users, using a range of techniques. For example Alpa is based on constraint solving, with current work attempting to more iteratively expose the search space (à la [3, 36])

#### 7 Conclusion

We have presented TOAST, a fully automatic partitioning system that leverages our novel named dimension analysis (NDA) to expose partitioning decisions to an MCTS agent, including the exploration or resolutions of sharding conflicts. We show by providing ahead-of-time propagation decisions and operating over the NDA our automatic partitioner is able to explore more performant solutions and achieve better results than other competing methods.

For future research, we will leverage NDA to train a model capable of predicting the optimal sharding immediately given set of colors to shard. This is achievable by training offline on many combinations of colors as the cost estimate from sharding sets of named dimensions should be deterministic.

#### References

- [1] Martín Abadi, Paul Barham, Jianmin Chen, Zhifeng Chen, Andy Davis, Jeffrey Dean, Matthieu Devin, Sanjay Ghemawat, Geoffrey Irving, Michael Isard, Manjunath Kudlur, Josh Levenberg, Rajat Monga, Sherry Moore, Derek G. Murray, Benoit Steiner, Paul Tucker, Vijay Vasudevan, Pete Warden, Martin Wicke, Yuan Yu, and Xiaoqiang Zheng. 2016. TensorFlow: A System for Large-Scale Machine Learning. In 12th USENIX Symposium on Operating Systems Design and Implementation (OSDI 16). USENIX Association, Savannah, GA, 265–283. https://www.usenix.org/conference/osdi16/technical-sessions/presentation/abadi
- [2] Sami Alabed, Daniel Belov, Bart Chrzaszcz, Juliana Franco, Dominik Grewe, Dougal Maclaurin, James Molloy, Tom Natan, Tamara Norman, Xiaoyue Pan, et al. 2024. Partir: Composing spmd partitioning strategies for machine learning. arXiv preprint arXiv:2401.11202 (2024).
- [3] Sami Alabed, Dominik Grewe, Juliana Franco, Bart Chrzaszcz, Tom Natan, Tamara Norman, Norman A. Rink, Dimitrios Vytiniotis, and Michael Schaarschmidt. 2022. Automatic Discovery of Composite SPMD Partitioning Strategies in PartIR. doi:10.48550/ARXIV. 2210.06352

- [4] Mohamed R Amer, Sinisa Todorovic, Alan Fern, and Song-Chun Zhu. 2013. Monte carlo tree search for scheduling activity recognition. In Proceedings of the IEEE international conference on computer vision. 1353–1360.
- [5] James Bradbury, Roy Frostig, Peter Hawkins, Matthew James Johnson, Chris Leary, Dougal Maclaurin, George Necula, Adam Paszke, Jake VanderPlas, Skye Wanderman-Milne, and Qiao Zhang. 2018. JAX: composable transformations of Python+NumPy programs. http: //github.com/google/jax
- [6] Cameron Browne, Edward Powley, Daniel Whitehouse, Simon Lucas, Peter I. Cowling, Stephen Tavener, Diego Perez, Spyridon Samothrakis, Simon Colton, and et al. 2012. A survey of Monte Carlo tree search methods. IEEE TRANSACTIONS ON COMPUTATIONAL INTEL-LIGENCE AND AI (2012).
- [7] Benjamin E Childs, James H Brodeur, and Levente Kocsis. 2008. Transpositions and move groups in Monte Carlo tree search. In 2008 IEEE Symposium On Computational Intelligence and Games. IEEE, 389–395.
- [8] Google Developers. 2023. Cloud TPU System Architecture. https://cloud.google.com/tpu/docs/system-architecture-tpu-vm. [Last updated 2023-11-06 UTC.].
- [9] Jonathan Godwin, Michael Schaarschmidt, Alexander L Gaunt, Alvaro Sanchez-Gonzalez, Yulia Rubanova, Petar Veličković, James Kirkpatrick, and Peter Battaglia. 2022. Simple GNN Regularisation for 3D Molecular Property Prediction and Beyond. In *International Conference on Learning Representations*. https://openreview.net/forum?id=1wVvweK3oIb
- [10] Google XLA team. 2017. XLA: Optimizing Compiler for Machine Learning. https://www.tensorflow.org/xla. https://www.tensorflow.org/xla
- [11] Yilin He, Chaojie Wang, Hao Zhang, Bo Chen, and Mingyuan Zhou. 2022. Edge Partition Modulated Graph Convolutional Networks. https://openreview.net/forum?id=ET1UAOYeU42
- [12] Jonathan Ho, Ajay Jain, and Pieter Abbeel. 2020. Denoising diffusion probabilistic models. Advances in Neural Information Processing Systems 33 (2020), 6840–6851.
- [13] Jordan Hoffmann, Sebastian Borgeaud, Arthur Mensch, Elena Buchatskaya, Trevor Cai, Eliza Rutherford, Diego de Las Casas, Lisa Anne Hendricks, Johannes Welbl, Aidan Clark, Tom Hennigan, Eric Noland, Katie Millican, George van den Driessche, Bogdan Damoc, Aurelia Guy, Simon Osindero, Karen Simonyan, Erich Elsen, Jack W. Rae, Oriol Vinyals, and Laurent Sifre. 2022. Training Compute-Optimal Large Language Models. doi:10.48550/ARXIV.2203.15556
- [14] Huimin Huang, Lanfen Lin, Ruofeng Tong, Hongjie Hu, Qiaowei Zhang, Yutaro Iwamoto, Xianhua Han, Yen-Wei Chen, and Jian Wu. 2020. Unet 3+: A full-scale connected unet for medical image segmentation. In ICASSP 2020-2020 IEEE international conference on acoustics, speech and signal processing (ICASSP). IEEE, 1055–1059.
- [15] Zhihao Jia, Matei Zaharia, and Alex Aiken. 2019. Beyond Data and Model Parallelism for Deep Neural Networks. In Proceedings of Machine Learning and Systems 2019, MLSys 2019, Stanford, CA, USA, March 31 - April 2, 2019, Ameet Talwalkar, Virginia Smith, and Matei Zaharia (Eds.), Vol. 1. mlsys.org, 1–13. https://proceedings.mlsys. org/book/265.pdf
- [16] Norm Jouppi, George Kurian, Sheng Li, Peter Ma, Rahul Nagarajan, Lifeng Nai, Nishant Patil, Suvinay Subramanian, Andy Swing, Brian Towles, et al. 2023. Tpu v4: An optically reconfigurable supercomputer for machine learning with hardware support for embeddings. In Proceedings of the 50th Annual International Symposium on Computer Architecture (Orlando, FL, USA) (ISCA '23). Association for Computing Machinery, New York, NY, USA, Article 82, 14 pages. doi:10.1145/3579371.3589350
- [17] Norman P. Jouppi, Doe Hyun Yoon, Matthew Ashcraft, Mark Gottscho, Thomas B. Jablin, George Kurian, James Laudon, Sheng Li, Peter Ma, Xiaoyu Ma, Thomas Norrie, Nishant Patil, Sushma Prasad, Cliff Young,

- Zongwei Zhou, and David Patterson. 2021. Ten Lessons From Three Generations Shaped Google's TPUv4i: Industrial Product. In 2021 ACM/IEEE 48th Annual International Symposium on Computer Architecture (ISCA) (Virtual Event, Spain) (ISCA '21). IEEE Press, 1–14. doi:10.1109/ISCA52012.2021.00010
- [18] Norman P. Jouppi, Cliff Young, Nishant Patil, David A. Patterson, Gaurav Agrawal, Raminder Bajwa, Sarah Bates, Suresh Bhatia, Nan Boden, Al Borchers, Rick Boyle, Pierre-luc Cantin, Clifford Chao, Chris Clark, Jeremy Coriell, Mike Daley, Matt Dau, Jeffrey Dean, Ben Gelb, Tara Vazir Ghaemmaghami, Rajendra Gottipati, William Gulland, Robert Hagmann, Richard C. Ho, Doug Hogberg, John Hu, Robert Hundt, Dan Hurt, Julian Ibarz, Aaron Jaffey, Alek Jaworski, Alexander Kaplan, Harshit Khaitan, Andy Koch, Naveen Kumar, Steve Lacy, James Laudon, James Law, Diemthu Le, Chris Leary, Zhuyuan Liu, Kyle Lucke, Alan Lundin, Gordon MacKean, Adriana Maggiore, Maire Mahony, Kieran Miller, Rahul Nagarajan, Ravi Narayanaswami, Ray Ni, Kathy Nix, Thomas Norrie, Mark Omernick, Narayana Penukonda, Andy Phelps, Jonathan Ross, Amir Salek, Emad Samadiani, Chris Severn, Gregory Sizikov, Matthew Snelham, Jed Souter, Dan Steinberg, Andy Swing, Mercedes Tan, Gregory Thorson, Bo Tian, Horia Toma, Erick Tuttle, Vijay Vasudevan, Richard Walter, Walter Wang, Eric Wilcox, and Doe Hyun Yoon. 2017. In-Datacenter Performance Analysis of a Tensor Processing Unit. CoRR abs/1704.04760 (2017). arXiv:1704.04760 http://arxiv.org/abs/1704.04760
- [19] Diederik P. Kingma and Jimmy Ba. 2015. Adam: A Method for Stochastic Optimization. In 3rd International Conference on Learning Representations, ICLR 2015, San Diego, CA, USA, May 7-9, 2015, Conference Track Proceedings, Yoshua Bengio and Yann LeCun (Eds.). http://arxiv.org/abs/1412.6980
- [20] Vijay Anand Korthikanti, Jared Casper, Sangkug Lym, Lawrence McAfee, Michael Andersch, Mohammad Shoeybi, and Bryan Catanzaro. 2023. Reducing activation recomputation in large transformer models. Proceedings of Machine Learning and Systems 5 (2023).
- [21] Chris Lattner, Mehdi Amini, Uday Bondhugula, Albert Cohen, Andy Davis, Jacques Pienaar, River Riddle, Tatiana Shpeisman, Nicolas Vasilache, and Oleksandr Zinenko. 2021. MLIR: Scaling Compiler Infrastructure for Domain Specific Computation. In 2021 IEEE/ACM International Symposium on Code Generation and Optimization (CGO). 2–14. doi:10.1109/CG051591.2021.9370308
- [22] Dmitry Lepikhin, HyoukJoong Lee, Yuanzhong Xu, Dehao Chen, Orhan Firat, Yanping Huang, Maxim Krikun, Noam Shazeer, and Zhifeng Chen. 2020. GShard: Scaling Giant Models with Conditional Computation and Automatic Sharding. CoRR abs/2006.16668 (2020). arXiv:2006.16668 https://arxiv.org/abs/2006.16668
- [23] Xupeng Miao, Yujie Wang, Youhe Jiang, Chunan Shi, Xiaonan Nie, Hailin Zhang, and Bin Cui. 2022. Galvatron: Efficient transformer training over multiple gpus using automatic parallelism. arXiv preprint arXiv:2211.13878 (2022).
- [24] Michael D. Moffitt and Pratik Fegade. 2025. The ASPLOS 2025 / EuroSys 2025 Contest on Intra-Operator Parallelism for Distributed Deep Learning. In Proceedings of the 30th ACM International Conference on Architectural Support for Programming Languages and Operating Systems, Volume 3 (Rotterdam, Netherlands) (ASPLOS '25). Association for Computing Machinery, New York, NY, USA, 5–17. doi:10.1145/3676642.3736399
- [25] Teresa Neto, Miguel Constantino, Isabel Martins, and João Pedro Pedroso. 2020. A multi-objective Monte Carlo tree search for forest harvest scheduling. European Journal of Operational Research 282, 3 (2020), 1115–1126.
- [26] Nvidia. 2023. NVIDIA A100 Tensor Core GPU. https://www.nvidia.com/en-gb/data-center/a100/. [Last updated 2023-11-06 UTC.].

- [27] Tesla NVIDIA. 2017. Nvidia® tesla® p100-the most advanced data center accelerator ever built. Technical report, Technical Report WP-08019-001 (2017).
- [28] OpenXLA. 2023. Shardy: A library for performing sharding computations. https://github.com/openxla/shardy.
- [29] OpenXLA. 2023. StableHLO: Backward compatible ML compute opset inspired by HLO/MHLO. https://github.com/openxla/ stablehlo. [Last updated 2023-11-06 UTC.].
- [30] Adam Paszke, Sam Gross, Francisco Massa, Adam Lerer, James Bradbury, Gregory Chanan, Trevor Killeen, Zeming Lin, Natalia Gimelshein, Luca Antiga, Alban Desmaison, Andreas Kopf, Edward Yang, Zachary DeVito, Martin Raison, Alykhan Tejani, Sasank Chilamkurthy, Benoit Steiner, Lu Fang, Junjie Bai, and Soumith Chintala. 2019. PyTorch: An Imperative Style, High-Performance Deep Learning Library. In Advances in Neural Information Processing Systems, H. Wallach, H. Larochelle, A. Beygelzimer, F. d'Alché Buc, E. Fox, and R. Garnett (Eds.), Vol. 32. Curran Associates, Inc. https://proceedings.neurips.cc/paper/2019/file/bdbca288fee7f92f2bfa9f7012727740-Paper.pdf
- [31] Reiner Pope, Sholto Douglas, Aakanksha Chowdhery, Jacob Devlin, James Bradbury, Jonathan Heek, Kefan Xiao, Shivani Agrawal, and Jeff Dean. 2023. Efficiently scaling transformer inference. Proceedings of Machine Learning and Systems 5 (2023).
- [32] Samyam Rajbhandari, Jeff Rasley, Olatunji Ruwase, and Yuxiong He. 2019. ZeRO: Memory Optimization Towards Training A Trillion Parameter Models. CoRR abs/1910.02054 (2019). arXiv:1910.02054 http://arxiv.org/abs/1910.02054
- [33] Olaf Ronneberger, Philipp Fischer, and Thomas Brox. 2015. U-net: Convolutional networks for biomedical image segmentation. In Medical image computing and computer-assisted intervention–MICCAI 2015: 18th international conference, Munich, Germany, October 5-9, 2015, proceedings, part III 18. Springer, 234–241.
- [34] Amr Sabry and Matthias Felleisen. 1992. Reasoning about programs in continuation-passing style.. In Proceedings of the 1992 ACM Conference on LISP and Functional Programming (San Francisco, California, USA) (LFP '92). Association for Computing Machinery, New York, NY, USA, 288–298. doi:10.1145/141471.141563
- [35] Alvaro Sanchez-Gonzalez, Jonathan Godwin, Tobias Pfaff, Rex Ying, Jure Leskovec, and Peter Battaglia. 2020. Learning to simulate complex physics with graph networks. In *International Conference on Machine Learning*. PMLR, 8459–8468.
- [36] Michael Schaarschmidt, Dominik Grewe, Dimitrios Vytiniotis, Adam Paszke, Georg Stefan Schmid, Tamara Norman, James Molloy, Jonathan Godwin, Norman Alexander Rink, Vinod Nair, et al. 2021. Automap: Towards ergonomic automated parallelism for ml models. arXiv preprint arXiv:2112.02958 2112.02958 (2021). arXiv:2112.02958 [cs.LG].
- [37] Noam Shazeer, Youlong Cheng, Niki Parmar, Dustin Tran, Ashish Vaswani, Penporn Koanantakool, Peter Hawkins, HyoukJoong Lee, Mingsheng Hong, Cliff Young, Ryan Sepassi, and Blake Hechtman. 2018. Mesh-TensorFlow: Deep Learning for Supercomputers. In Neural Information Processing Systems.

- [38] Mohammad Shoeybi, Mostofa Patwary, Raul Puri, Patrick LeGresley, Jared Casper, and Bryan Catanzaro. 2019. Megatron-LM: Training Multi-Billion Parameter Language Models Using Model Parallelism. CoRR abs/1909.08053 (2019). arXiv:1909.08053 http://arxiv.org/abs/1909.08053
- [39] David Silver, Thomas Hubert, Julian Schrittwieser, Ioannis Antonoglou, Matthew Lai, Arthur Guez, Marc Lanctot, Laurent Sifre, Dharshan Kumaran, Thore Graepel, et al. 2017. Mastering chess and shogi by self-play with a general reinforcement learning algorithm. arXiv preprint arXiv:1712.01815 (2017).
- [40] Marc Snir, Steve W. Otto, David W. Walker, Jack Dongarra, and Steven Huss-Lederman. 1995. MPI: The Complete Reference. MIT Press, Cambridge, MA, USA.
- [41] Jianlin Su, Murtadha Ahmed, Yu Lu, Shengfeng Pan, Wen Bo, and Yunfeng Liu. 2024. Roformer: Enhanced transformer with rotary position embedding. *Neurocomputing* 568 (2024), 127063.
- [42] Gemma Team, Thomas Mesnard, Cassidy Hardin, Robert Dadashi, Surya Bhupatiraju, Shreya Pathak, Laurent Sifre, Morgane Rivière, Mihir Sanjay Kale, Juliette Love, et al. 2024. Gemma: Open models based on gemini research and technology. arXiv preprint arXiv:2403.08295 (2024).
- [43] Colin Unger, Zhihao Jia, Wei Wu, Sina Lin, Mandeep Baines, Carlos Efrain Quintero Narvaez, Vinay Ramakrishnaiah, Nirmal Prajapati, Pat McCormick, Jamaludin Mohd-Yusof, Xi Luo, Dheevatsa Mudigere, Jongsoo Park, Misha Smelyanskiy, and Alex Aiken. 2022. Unity: Accelerating DNN Training Through Joint Optimization of Algebraic Transformations and Parallelization. In 16th USENIX Symposium on Operating Systems Design and Implementation (OSDI 22). USENIX Association, Carlsbad, CA, 267–284. https://www.usenix.org/conference/osdi22/presentation/unger
- [44] Ashish Vaswani, Noam Shazeer, Niki Parmar, Jakob Uszkoreit, Llion Jones, Aidan N. Gomez, Lukasz Kaiser, and Illia Polosukhin. 2017. Attention Is All You Need. CoRR abs/1706.03762 (2017). arXiv:1706.03762 http://arxiv.org/abs/1706.03762
- [45] Yuanzhong Xu, HyoukJoong Lee, Dehao Chen, Blake A. Hechtman, Yanping Huang, Rahul Joshi, Maxim Krikun, Dmitry Lepikhin, Andy Ly, Marcello Maggioni, Ruoming Pang, Noam Shazeer, Shibo Wang, Tao Wang, Yonghui Wu, and Zhifeng Chen. 2021. GSPMD: General and Scalable Parallelization for ML Computation Graphs. CoRR abs/2105.04663 (2021). arXiv:2105.04663 https://arxiv.org/abs/2105.04663
- [46] Yanli Zhao, Andrew Gu, Rohan Varma, Liang Luo, Chien-Chin Huang, Min Xu, Less Wright, Hamid Shojanazeri, Myle Ott, Sam Shleifer, et al. 2023. Pytorch FSDP: experiences on scaling fully sharded data parallel. arXiv preprint arXiv:2304.11277 16, 12 (Aug. 2023), 3848–3860. doi:10.14778/3611540.3611569
- [47] Lianmin Zheng, Zhuohan Li, Hao Zhang, Yonghao Zhuang, Zhifeng Chen, Yanping Huang, Yida Wang, Yuanzhong Xu, Danyang Zhuo, Joseph E. Gonzalez, and Ion Stoica. 2022. Alpa: Automating Interand Intra-Operator Parallelism for Distributed Deep Learning. CoRR abs/2201.12023 (July 2022), 559–578. arXiv:2201.12023 https:// arxiv.org/abs/2201.12023